DEPARTMENT OF THE INTERIOR
U.S. GEOLOGICAL SURVEY

PREPARED IN COOPERATION WITH THE SAUDI ARABIAN DEPUTY MINISTRY FOR PETROLEUM AND MINERAL RESOURCES

MISCELLANEOUS FIELD STUDIES
MAP MF-2129

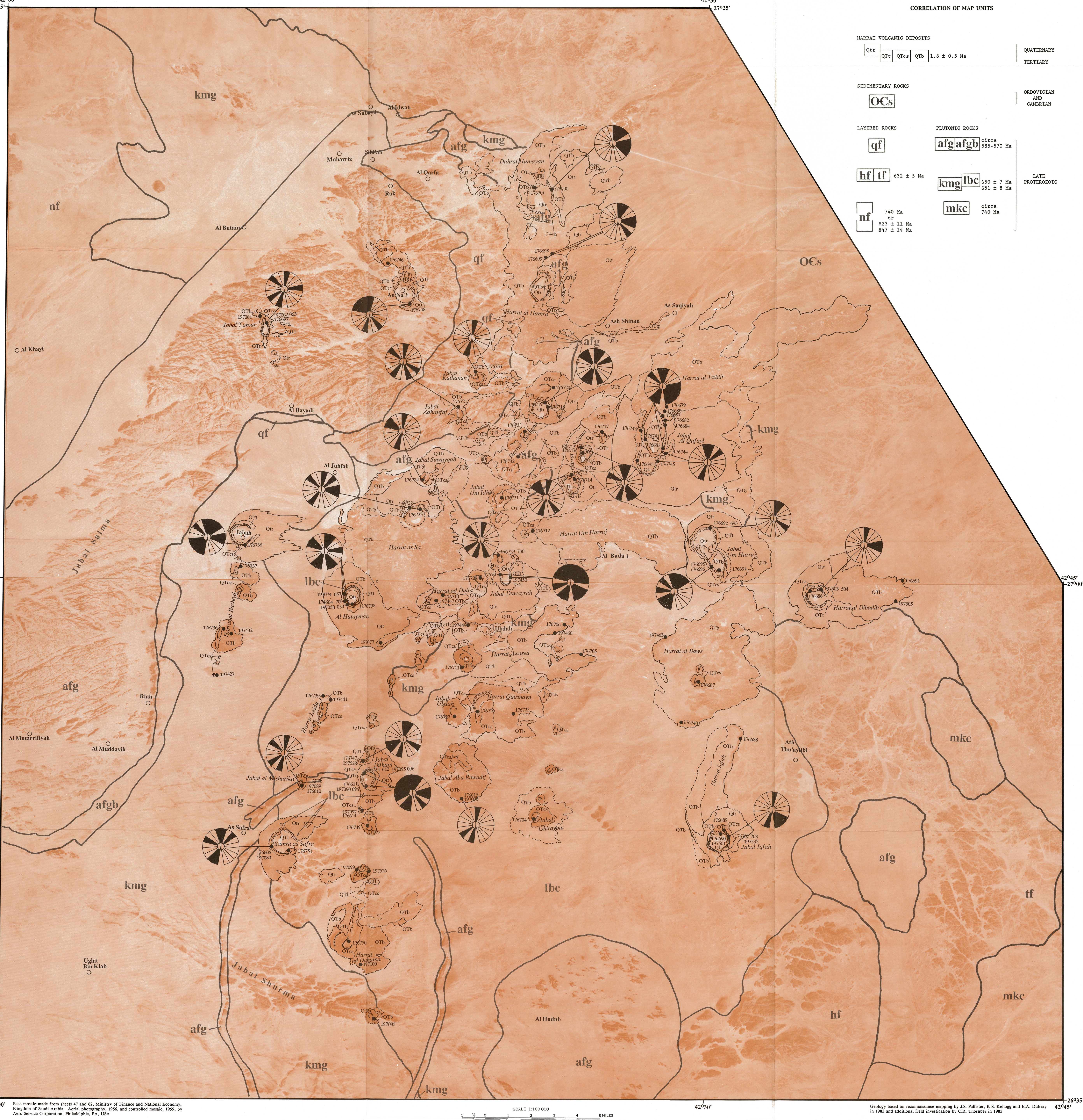

Base mosaic made from sheets 47 and 62, Ministry of Finance and National Economy, Kingdom of Saudi Arabia. Aerial photography, 1956, and controlled mosaic, 1959, by Aero Service Corporation, Philadelphia, PA, USA

SCALE 1:100 000

1 ½ 0 1 2 3 4 5 MILES

1 .5 0 1 2 3 4 5 KILOMETERS

Geology based on reconnaissance mapping by J.S. Pallister, K.S. Kellogg and E.A. DuBray in 1983 and additional field investigation by C.R. Thornber in 1985

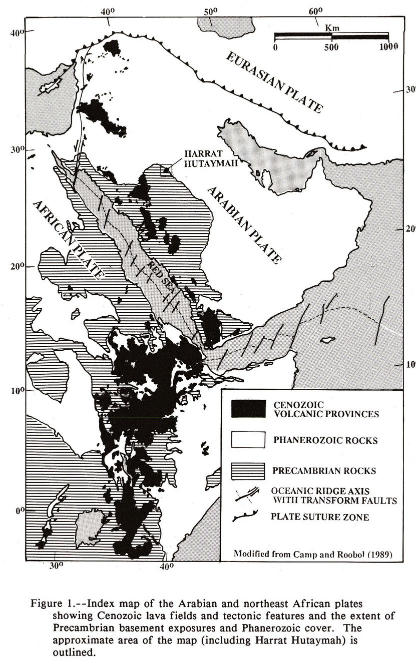

Figure 1.--Index map of the Arabian and northeast African plates showing Cenozoic lava fields and tectonic features and the extent of Precambrian basement exposures and Phanerozoic cover. The approximate area of the map (including Harrat Hutaymah) is outlined.

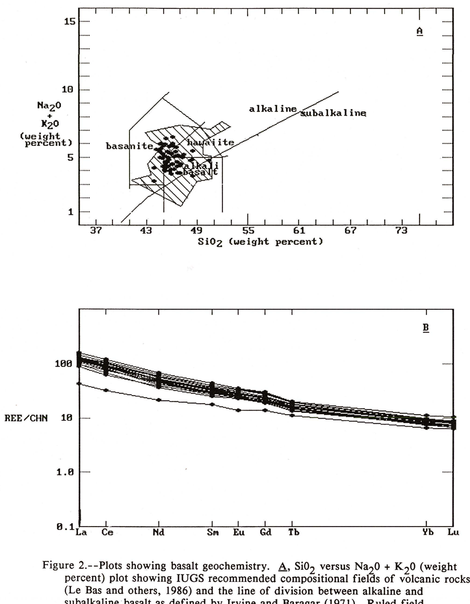

Figure 2.--Plots showing basalt geochemistry. A, SiO_2 versus $Na_2O + K_2O$ (weight percent) plot showing IUGS recommended compositional fields of volcanic rocks (Le Bas and others, 1986) and the line of division between alkaline and subalkaline basalt as defined by Irvine and Baragar (1971). Ruled field corresponds to the range of Arabian Cenozoic basaltic lavas (from Coleman and others, 1983), and points represent 60 basalt samples from Harrat Hutaymah (Electron probe analyses of fused glass); B, Log plot of rare-earth element (REE) abundances (normalized to chondritic (CHN) values) for 26 representative basalt samples from Harrat Hutaymah.

GEOLOGIC MAP OF HARRAT HUTAYMAH, WITH PETROLOGIC CLASSIFICATION AND DISTRIBUTION OF ULTRAMAFIC INCLUSIONS, SAUDI ARABIA

By
Carl R. Thornber
1990

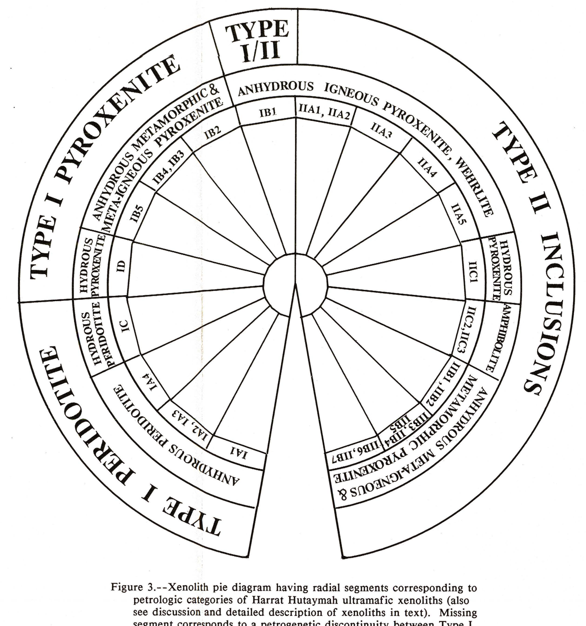

Figure 3.--Xenolith pie diagram having radial segments corresponding to petrologic categories of Harrat Hutaymah ultramafic xenoliths (also see discussion and detailed description of xenoliths in text). Missing segment corresponds to a petrogenetic discontinuity between Type I "host mantle" peridotite and the petrologic continuum of metamorphic, meta-igneous, metasomatic, and igneous varieties of Type II inclusions and Type I pyroxenite observed in the Hutaymah xenolith suite.

EXPLANATION FOR FIGURE 3

Type I peridotite
- Subtype IA--Anhydrous spinel peridotite
  - IA1 Protogranular and porphyroclastic spinel lherzolite
  - IA2 Tectonized spinel lherzolite
  - IA3 Equigranular spinel lherzolite
  - IA4 Spinel harzburgite
- Subtype IC--Hydrous peridotite
  - IC Hydrous-phase bearing peridotite, undivided

Type I pyroxenite
- Subtype ID--Hydrous pyroxenite
  - ID Hydrous-phase bearing pyroxenite, undivided
- Subtype IB--Anhydrous metamorphic and meta-igneous pyroxenite
  - IB5 Orthopyroxenite
  - IB4 Olivine websterite
  - IB3 Websterite and clinopyroxenite
  - IB2 Clinopyroxene megacryst (discrete or relict)

Type I/Type II transitional anhydrous igneous pyroxenite
- IB1 Transitional clinopyroxenite, undivided

Type II xenoliths
- Subtype IIA--Anhydrous igneous pyroxenite and wehrlite
  - IIA1 Clinopyroxene megacrysts
  - IIA2 Clinopyroxenite
  - IIA3 Wehrlite and olivine-rich clinopyroxenite
  - IIA4 Websterite
  - IIA5 Fe-rich clinopyroxenite
- Subtype IIC--Hydrous xenoliths and megacrysts
  - IIC1 Amphibole clinopyroxenite
  - IIC2 Amphibole megacrysts
  - IIC3 Amphibolite
- Subtype IIB--Anhydrous meta-igneous and metamorphic pyroxenite
  - IIB1 Websterite
  - IIB2 Orthopyroxenite
  - IIB3 Green-spinel websterite
  - IIB4 Green-spinel olivine websterite
  - IIB5 Green-spinel plagioclase websterite
  - IIB6 Green-spinel garnet pyroxenite
  - IIB7 Garnet pyroxenite

CORRELATION OF MAP UNITS

HARRAT VOLCANIC DEPOSITS

Qtr | QTt | QTcs | QTb — 1.8 ± 0.5 Ma — QUATERNARY / TERTIARY

SEDIMENTARY ROCKS

OЄs — ORDOVICIAN AND CAMBRIAN

LAYERED ROCKS

qf

hf | tf — 632 ± 5 Ma

nf — 740 Ma or 823 ± 11 Ma, 847 ± 14 Ma

PLUTONIC ROCKS

afg | afgb — circa 585-570 Ma

kmg | lbc — 650 ± 7 Ma, 651 ± 8 Ma

mkc — circa 740 Ma

LATE PROTEROZOIC

DESCRIPTION OF MAP UNITS

QUATERNARY AND TERTIARY VOLCANIC UNITS

Qtr **Reworked alkali basaltic tuff (Quaternary)**--Aprons of unconsolidated, tan to reddish-brown tuffaceous sand and silt overlying alkali basaltic tuff ring deposits (unit QTt) and adjacent country rock. Found as thin-bedded deposits (reworked in situ) and as channel deposits on the flanks of tuff rings. Basaltic and crustal xenoliths and ultramafic xenoliths or xenocrysts associated with reworked tuff are found as surficial lag deposits near crater rims or in small erosional channels within the tuff-ring flanks

QTt **Alkali basaltic tuff-ring deposits (Quaternary and Tertiary)**--Poorly consolidated, massive to bedded layers of gray-brown to red-brown basaltic tephra that dip 5°-15° away from a central crater and form tuff-rings. Tephra deposits often include minor cinder deposits and spattery basaltic flows. Tuff varies from fine-grained, massive beds (as much as 5 m thick) to well-bedded and crossbedded tuff-matrix conglomerate and coarse-grained lapilli tuff. Inversely graded beds are common within tuffaceous conglomerate units. Tuff-matrix conglomerate and lapilli tuff associated with different vents or within multiple vent complexes, contain a highly variable size range and population of crustal basement xenoliths, basalt xenoliths, and ultramafic xenoliths and xenocrysts

QTcs **Alkali basaltic cinder and spatter (Quaternary and Tertiary)**--Unconsolidated to poorly consolidated and variably agglutinated alkali basaltic cinder, bomb, and spatter deposits, which make up and are proximal to volcanic cones and fissure vents. Cinder cones contain black to reddish-brown (oxidized) cinder-scoria deposits, generally having greater than 30° slope angles, and are symmetrical, asymmetrical, or flow-breached. There is complete gradation among cinder and cinder-spatter cones and discontinuous spatter ramparts which define elongate fissure vents. Strings of cinder cones and fissure vents define north-trending lineaments in the central area of the field. Cinder cones also occur in association with explosive vent complexes of tuff-rings (both pre-tuff ring and post-tuff ring associations are observed). Type II megacrysts and xenoliths are common but not ubiquitous; crustal basement xenoliths are rare, and Type II peridotite and pyroxenite xenoliths are very rare

QTb **Alkali basalt flow (Quaternary and Tertiary)**--Olivine phyric and microphyric alkali olivine basalt (and basanite) flows. Nonvesicular or slightly vesicular and commonly diktytaxitic, with intergranular to intersertal textures. Less common pilotaxitic, glomeroporphyritic, and coarse subophitic flows are present and minor calcification is common. Flows emanate from breached cinder and(or) spatter cones or elongate fissures and range in thickness from 2-m-thick single flow units to as much as 40-m-thick flow sequences. Some basalt is devoid of xenocrystic or xenolithic inclusions. Overall relative abundances of inclusions are: Type II megacrysts > Type II xenoliths > Type I xenoliths. Basement crustal xenoliths are dominant in some flows but absent in most

PALEOZOIC SEDIMENTARY ROCKS

OЄs **Saq Sandstone (Ordovician and Cambrian)**--Moderately well sorted, massively bedded quartz arenite (Johnson and Williams, 1984)

LATE PROTEROZOIC LAYERED ROCKS

qf **Quarfa formation**--Porphyritic rhyolite lava, ash-flow tuff, and sparse volcaniclastic conglomerate at the northeast margin of Jabal Salma are interpreted as caldera-fill deposits associated with the alkali granite plutonic suite (unit afg) at Jabal Salma (Kellogg, 1985)

hf **Hibshi formation**--Intertongued clastic sediment of volcanic and plutonic provenance; volcanic units are dominated by subaerial dacitic to andesitic extrusives and minor amounts of basaltic extrusives (Pallister, 1984). Formation is metamorphosed to zeolite or greenschist facies (Johnson and Williams, 1984). A zircon U-Pb date of 632 ± 5 Ma is reported by Cole and Hedge (1986) on a sample of welded tuff about 100 m above the unconformable base

tf **Turmus formation**--Interbedded andesitic flows and tuffs, subordinate lithic graywacke, and minor conglomerate. Concentrations of hypabyssal rhyolitic dikes and sills are present (Johnson and Williams, 1984). This unit is interpreted as broadly contemporaneous with the Hibshi Formation (Johnson and Williams, 1984; Cole and Hedge, 1986)

nf **Nuf formation**--Metamorphosed basalt (locally has pillow structure), andesite, dacite, rhyolite, rhyodacite, minor marble, and sparse graywacke. Metamorphic grade is predominantly greenschist to lower amphibolite facies (Kellogg, 1984). A 740 Ma age has been estimated by regional correlation with K-Ar dated Hulayfah group layered rocks (about 200 km southwest of Harrat Hutaymah) (Kellogg, 1984; Vaslet and others, 1987; Cole and Hedge, 1986; Quick and Doebrich, 1987). Current evidence cannot rule out the possibility that this unit may be correlated with ophiolitic rocks at Bir Tuluhah (200 km southwest of Harrat Hutaymah), dated by U-Pb (zircon) at 823 ± 11 Ma and 847 ± 14 Ma (Pallister and others, 1988; Quick and Bosch, 1989)

LATE PROTEROZOIC PLUTONIC ROCKS

afg **Alkali-feldspar granite suite**--Plutons and ring structures of light-gray to pink, medium- to coarse-grained, allotriomorphic to hypidiomorphic granular biotite alkali-feldspar granite, muscovite-bearing alkali-feldspar granite, sodic amphibole-bearing alkali feldspar granite, and alkali-feldspar quartz syenite granophyre (Johnson and Williams, 1984). A Rb-Sr age of 580 ± 5 Ma was determined for the Jabal Salma pluton and caldera complex (unit afgb) (Stuckless and others, 1984). Unit afg intrusives of the Harrat Hutaymah area are included in the Abanat suite of peralkaline, peraluminous, and metaluminous granite emplaced in the northeastern Arabian Shield during the interval between 585 and 570 Ma (Cole and Hedge, 1986). In general, this suite is considered to be part of a broadly cogenetic series of undeformed, circular, postorogenic granite plutons that occur throughout the Arabian-Nubian Shield and range in age from about 620 to 550 Ma (Stoeser and Elliott, 1980; Pallister, 1984; Kellogg, 1985)

afgb **Alkali-feldspar granite border**--The border zone southeast of Jabal Salma (unit afg) comprises a distinct rim of hornblende quartz orthoclase syenite, interpreted as coeval with a biotite orthoclase granite member of the Salma plutonic suite (Kellogg, 1985)

kmg **Kilab monzogranite**--Unit comprises numerous batholithic intrusives of light-to pinkish-gray, massive to weakly foliated, medium-grained biotite monzogranite and is regionally heterogeneous, grading into hornblende-biotite granodiorite or fine-grained porphyritic biotite syenogranite (Cole and Hedge, 1986; Pallister, 1984; Johnson and Williams, 1984). Intruded by northwest- and northeast-trending dikes of rhyolite and diabase (not shown on map) that do not intrude younger alkali-feldspar granite (unit afg) plutons. More mafic rocks of the Laban complex (unit lbc) are intruded by Kilab (Pallister, 1984). However, the 651 ± 8 Ma zircon U-Pb age of Kilab monzogranite is analytically indistinguishable from the Laban diorite complex zircon U-Pb age of 650 ± 7 Ma (Cole and Hedge, 1986), indicating that the intrusive suites that make up most of the crustal basement rock of Harrat Hutaymah were nearly contemporaneous

lbc **Laban complex**--Intrusive complex consisting of variably deformed and metamorphosed biotite quartz diorite, biotite and(or) hornblende diorite and tonalite, hornblende and pyroxene gabbro and monzogabbro, and subordinate granodiorite. Metamorphic grade is predominantly amphibolite facies. Intruded by plutons of Kalab monzogranite (unit kmg) and overlain by the Hibshi formation (unit hf) (Pallister, 1984). Dated by Pb-U zircon at 650 ± 7 Ma (Cole and Hedge, 1986)

mkc **Makhul complex**--Intrusive complex composed of grayish-black, locally gneissic, extremely heterogeneous quartz diorite, granodiorite, and subordinate gabbro, quartz monzodiorite quartz monzonite, tonalite, and monzogranite (Johnson and Williams, 1984). A circa 740 Ma age (Cole and Hedge, 1986) is based on similarity with the old "island arc" intrusive rocks of the Juwayy Rashib complex (about 80 km west of Harrat Hutaymah, Quick and Doebrich, 1987). Sodic granodiorite from that complex was dated at 738 ± 2 Ma (Hedge, written communication, 1985)

Crater rim of tuff ring or cinder and(or) spatter cone--Hachures point toward depression

Contact (harrat volcanic units)--Long dashed where partially exposed; short dashed where covered by Quaternary alluvium. Relative ages indicated where discernable by y, younger; o, older

Contact (crustal basement rocks)--Exposed and unexposed

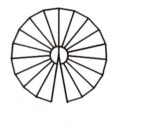

Xenolith pie diagram--Segments correspond to petrologic categories of ultramafic xenoliths (see fig. 3). The presence of a particular xenolith type at a given locality is indicated by a filled pie segment

176738 • **Sample locality**--176*** = Thornber, this investigation; 197*** = Pallister, 1984

Tabah ○ **Town or village**

Harrat Um Harruj **Place name relating to Harrat volcanic deposits**--"Harrat" indicates region of volcanic vents and deposits; "Jabal" indicates specific cones or topographically high features associated with multiple vent complexes; and "Samra" indicates a ring structure

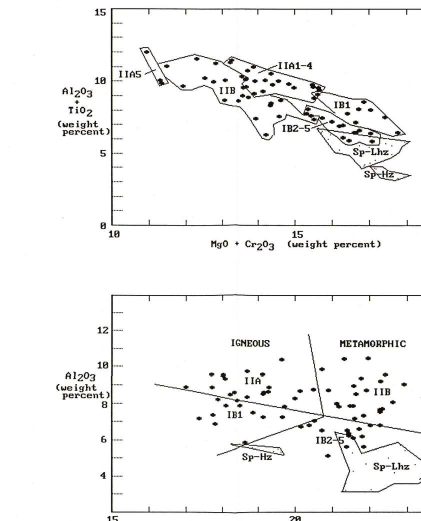

Figure 4.--Plots showing compositions of clinopyroxene in Hutaymah anhydrous pyroxenite (Electron microprobe analyses by author using ARL-SEMQ facilities at USGS, Reston and Denver). Fields of spinel lherzolite and spinel harzburgite clinopyroxene compositions are labeled Sp-Lhz and Sp-Hz, respectively. Data points represent average clinopyroxene-core analyses from different samples. Field boundaries are based on Hutaymah xenolith subtypes (xenolith subtype symbols described in text; also see fig. 3). A, Plot of $MgO + Cr_2O_3$ versus $Al_2O_3 + TiO_2$; B, Plot of CaO versus Al_2O_3.

INTRODUCTION

This map shows detailed geology of the Quaternary and Tertiary volcanic deposits that comprise Harrat Hutaymah and an updated and generalized compilation of the underlying Proterozoic and Paleozoic basement rocks. Quaternary alluvial cover and details of basement geology (that is, faults, dikes and other features) are not shown.

Volcanic unit descriptions and contact relations are based upon field investigation by the author and on compilation and revision of mapping by Kellogg (1984; northern half of area) and Pallister (1984; southern half of area). A single K-Ar date of 1.80 ± 0.05 Ma for an alkali olivine basalt flow transected by the Al Hutaymah tuff ring (Pallister, 1984) provides the basis for an estimated late Tertiary to Quaternary age range for all harrat volcanic units other than unit Qtr (tuff reworked during Quaternary time). Contact relations and unit descriptions for the basement rocks were compiled from Pallister (1984), Kellogg (1984 and 1985), DuBray (1984), Johnson and Williams (1984), Vaslet and others (1987), Cole and Hedge (1986), and Richter and others (1984). All rock unit names in this report are informal and capitalization follows Saudi Arabian stratigraphic nomenclature (Fitch, 1980). Geographic information was compiled from Pallister (1984), Kellogg (1984), and Fuller (in Johnson and Williams, 1984) and from field investigation by the author in 1986.

The pie diagrams on the map show the distribution and petrology of ultramafic xenoliths of Harrat Hutaymah. The pie diagrams are explained by a detailed classification of ultramafic xenoliths that is introduced in this report.

REGIONAL GEOLOGIC SETTING--THE RED SEA RIFT AND WESTERN ARABIA

One of the world's largest alkali basalt provinces covers an area of 180,000 km^2 within the Arabian Plate (Camp and others, 1987) (fig. 1). This extensive volcanic field is temporally and spacially related to Cenozoic rifting of Africa and Arabia. Proterozoic oceanic-arc and continental-margin-arc accretionary mechanisms (about 900 Ma to 600 Ma) are generally accepted for the formation of the Arabian-Nubian Shield (Stoeser and Camp, 1985; Quick and Bosch, 1989). Postorogenic granite was emplaced throughout the shield from 670 Ma to 550 Ma (Stoeser and Elliott, 1980), and the region persisted as a stable craton throughout most of Paleozoic and Mesozoic time. Subalkaline-alkaline magmatism associated with initial stages of crustal attenuation of the proto-Red Sea region may have begun as early as Eocene time (Pallister, 1987). The majority of rift-related volcanism in the region has occurred from at least Oligocene time to the present (Coleman and others, 1977, 1983; Coleman, 1984). Tholeiitic basalt, similar to mid-ocean ridge basalt (MORB), has been erupted in the axial trough of the southern Red Sea during the last 5 m.y. (Cochran, 1983). An asymmetric distribution of volcanism marginal to the Red Sea oceanic spreading center is apparent from the absence of volcanic activity north of lat 15° N. in east Africa, in contrast to extensive basaltic volcanism in western Saudi Arabia. Spacially distinct harrats of the western Arabian peninsula occur in a north-northwest-trending physiographic array that is subparallel to the Red Sea (fig. 1). ("Harrat" is the possessive form of the Arabic word "harra," which means "stony area, volcanic country or lava field," and is related to the adjective "harr," meaning "hot" (Camp and Roobol, 1989). The term "harrat" is used synonymously with "alkali basalt field" by Arabian geologists.) These harrats are contemporaneous with early rifting and active spreading of the Red Sea and comprise predominantly alkali-olivine basalt (fig. 2a). Available radiometric data for basalt of western Arabia and heat-flow data acquired along a seismic-refraction traverse perpendicular to the Red Sea axis in Saudi Arabia reflect the northeasterly expansion of a mantle thermal anomaly away from the present location of the Red Sea spreading axis (Gettings, written communication, 1989).

SIGNIFICANCE OF HARRAT HUTAYMAH

Harrat Hutaymah is the youngest harrat (less than 2 Ma; Pallister, 1984) in Saudi Arabia. Located at the northeast margin of the Arabian Shield, it is the most distal harrat from the Red Sea axis (fig. 1). Volcanic deposits from single- or multiple-vent eruptive centers cover about 900 km^2 and are scattered over about a 2500 km^2 area. Harrat Hutaymah is small compared to other Cenozoic basalt fields in Arabia, but it contains the largest proportion of exposed basaltic tephra deposits. The basaltic tephras were deposited as annular tuff rings, are usually rich in mantle inclusions, and probably resulted from explosive diatreme eruption of mantle-derived magmas. Basalt is basanitic to alkali-olivine basaltic in composition and has enriched rare-earth-element compositions (fig. 2). The population of upper mantle inclusions hosted by Hutaymah tephras and basalt flows includes most of the varieties that occur in alkali basalt fields throughout the world. The diversity of ultramafic xenoliths from Harrat Hutaymah (this investigation) is much greater than from other Arabian harrats (Coleman and others, 1983; Ghent and others, 1980; McGuire, 1988). This relatively juvenile harrat provides a clear record of initial explosive stages of magmatism, in contrast to older basalt fields where early explosive deposits were buried by subsequent lava flows. Because the field is young and isolated, it provides mantle melts that have traversed and entrained nodules of a more "pristine" section of the Arabian lithospheric mantle; that is, subcontinental lithosphere that has not been affected by the transit of numerous earlier melt batches).

ULTRAMAFIC XENOLITH NOMENCLATURE

In general, ultramafic xenoliths in continental alkaline volcanic rocks are referred to as mantle xenoliths. These xenoliths are samples of the lithospheric mantle that has been variably affected by tectonic and magmatic processes related to the generation, propagation, and infiltration of host magmas. Xenolith rock-names are from the classification scheme of Streckeisen (1973) for ultramafic rocks. The terms "Type I" and "Type II" are consistent with nomenclature established by Wilshire and Shervais (1975) and Frey and Prinz (1978) for two petrogenetically distinct varieties of mantle xenoliths that are found in alkali basalt. Type I inclusions are typically green and are Cr and Mg rich and Al, Ti, and Fe poor relative to Type II xenoliths. Spinel-lherzolite is the most common of the Type I xenoliths in alkali-basalt and represents the major constituent of the upper mantle that was traversed and intermittently sampled by host magmas. Chrome-diopside pyroxenite and spinel harzburgite make up a significant proportion of this category. Garnet periodotite is extremely rare in alkali-basalt volcanic provinces and does not occur at Harrat Hutaymah. Type II inclusions, generally black, are mostly varieties of aluminous-augite pyroxenite, which are generally considered as cogenetic with either the host magma or with precursory alkaline magmas.

The textural terminology applied to ultramafic xenoliths (other than general textural terminology for igneous rocks) is based upon a combination of terms suggested by Harte (1977 and 1983), Mercier and Nicholas (1975), and Nielson-Pike and Schwarzman (1977).

HUTAYMAH ULTRAMAFIC XENOLITH AND MEGACRYST SUITE

A representative sampling of about 600 ultramafic xenoliths and megacrysts was made from all xenolith-rich alkali-basalt flows and tephras of Harrat Hutaymah. This suite comprises a wide variety of peridotite and pyroxenite, both with and without primary or secondary hydrous phases. The relative abundance of Type I and Type II xenoliths from any given locality varies with the volcanic host (basalt or basaltic-tuff) and may vary among successive deposits of individual vents or between similar deposits associated with multiple-vent complexes. Both types of inclusions are abundant over the entire volcanic field and numerous inter-type and intra-type "composite" xenoliths have been sampled. The texture, modal mineralogy, and mineral chemistry are significantly variable within each general category and provide the basis for more detailed petrologic classification of primary variants within each type and for the definition of a transitional Type I/Type II category (fig. 3). The term "primary" is used here to mean that inclusion types represent material equilibrated under conditions at the xenolith source. Late-stage reaction products and textures (other than metasomatism), which are associated with depressurization or heating during transport or emplacement, are not used to define xenolith subtypes. Likewise, products of postdepositional alteration are not considered in the classification scheme presented here.

GENERAL DESCRIPTION AND OCCURRENCE OF HUTAYMAH TYPE I XENOLITHS AND MEGACRYSTS

Inclusions are lherzolite, harzburgite, and pyroxenite. Spinel lherzolite is the most common of the Type I xenoliths and is composed of 45-75 percent olivine, 15-40 percent orthopyroxene, 5-14 percent clinopyroxene, and 1-5 percent spinel. In alkali olivine basalt flows, xenoliths range in size from less than 1 cm fragments to 5 cm rounded inclusions. In most alkali basaltic tuff deposits, spinel lherzolite occurs as small, irregular, disaggregated fragments and as rounded or ovoid xenoliths as much as 30 cm in diameter. Type I spinel lherzolite displays a gradational range of petrologic characteristics indicating various degrees of deformation, subsolidus equilibration, episodic re-equilibration, and metasomatic fluid interaction. Evidence of partial melting is commonly observed in less abundant, generally smaller xenoliths of clinopyroxene-poor lherzolite and harzburgite. Rare hydrous peridotite contains amphibole or mica in both equilibrated and secondary textural associations. Type I pyroxenite inclusions are almost exclusively found in basaltic tuff ring deposits. Discrete samples range from small (1-5 cm) megacrysts of exsolved clinopyroxene and rare orthopyroxene megacrysts to large (15 cm) round websterite xenoliths. Pyroxenite is also in veins (1-2 cm thick) either crosscutting porphyroclastic spinel lherzolite or concordant with foliation in tectonized lherzolite. Type I pyroxenite is composed of clinopyroxenite, websterite, olivine websterite, and orthopyroxenite with less common primary or secondary hydrous-phase-bearing pyroxenite. Clinopyroxene of Type I xenoliths is all of the Ca-rich, emerald-green, "Cr-diopside" variety. In Type I pyroxenite, clinopyroxene is generally more enriched in aluminum and titanium than Type I peridotite clinopyroxene (fig. 4A).

Type I classification

Type I inclusions are grouped into subtypes IA (peridotite) and Type IB (pyroxenite) on the basis of modal mineralogy. These are not equivalent to Type IA and Type IB peridotite of Menzies (1983), which correspond to metasomatized and unmetasomatized peridotite and are identified on the basis of rare-earth-element concentrations in clinopyroxene. Subtypes IA and IB are further divided based upon modal and textural criteria. Subtypes IC and ID refer to hydrous-phase bearing Type I peridotite and pyroxenite, respectively. General characteristics of Type I xenoliths follow.

Type I peridotite

Subtype IA--Anhydrous spinel peridotite

IA1 Protogranular and porphyroclastic spinel lherzolite--There is complete gradation between protogranular (rare) and coarse porphyroclastic (common) textures. Protogranular rocks contain kink-banded olivine and variably deformed grains of orthopyroxene (both greater than 4 mm and having irregular-curvilinear grain boundaries) and intergranular (less than 2 mm) anhedral clinopyroxene and accessory brown spinel. Porphyroclastic rocks contain large (3-8 mm) porphyroclasts of olivine and orthopyroxene amidst a variably developed matrix of neoblastic to mosaic olivine, orthopyroxene, clinopyroxene, and brown spinel. Textures grade into tectonized (IA2) or equigranular (IA3).

IA2 Tectonized spinel lherzolite--Porphyroclastic with predominant laminar, foliated, fluidal, and disruptive textures; secondary granulation and neoblastic recrystallization are developed within layers concordant with foliation.

IA3 Equigranular spinel lherzolite--Tabular- to mosaic-equigranular intergrowth of less than 2 mm olivine and orthopyroxene with randomly distributed clinopyroxene and rounded to xenomorphic brown spinel at grain junctions. Coarse (4 mm) equigranular textures are present in samples having relict porphyroclasts and having overall textures that are gradational from equigranular toward IA1 and IA2.

IA4 Spinel harzburgite--Porphyroclastic to secondary granuloblastic or coarse-grained allotriomorphic-granular. Clinopyroxene and spinel typically show evidence of partial melting.

Subtype IC--Hydrous peridotite

IC Hydrous-phase bearing peridotite, undivided--Variants include (1) IA2 and IA3 lherzolite having as much as 7 percent of late-stage, 1-3 mm xenomorphic amphibole (pargasite ?) that may enclose spinel and, in some samples, trace amounts of less than 1 mm subhedral phlogopite within and adjacent to pyroxene, (2) IA1, IA2, IA3, and IA4 peridotite having amphibole or mica along intragranular fractures and cracks and in pervasive veinlets, and (3) IA1 and IA2 lherzolite having secondary intergranular kaersutitic amphibole (in reaction coronas adjacent to Type IIC amphibolite veins).

Type I pyroxenite

Subtype ID--Hydrous pyroxenite

ID Hydrous-phase bearing pyroxenite, undivided--Variants include (1) allotriomorphic-granular phlogopite clinopyroxenite having about 50 percent each of phlogopite and clinopyroxene, (2) IB3 websterite having less than 1 percent phlogopite within and adjacent to exsolved pyroxene grains, and (3) amphibole or mica along intragranular and intracrystalline fractures and cracks in IB5 orthopyroxenite.

Subtype IB--Anhydrous metamorphic and meta-igneous pyroxenite

IB5 Orthopyroxenite--Discrete xenoliths are usually small (as much as 4 cm) and range in texture from coarse-grained allotriomorphic to coarse-grained mosaic-equigranular. Clinopyroxene occurs as less than 1 mm size xenomorphic crystals between 3-5 mm subhedral or euhedral orthopyroxene crystals. Orthopyroxene typically has finely exsolved cores and exsolution-free rims. Rare orthopyroxene megacrysts (2 cm) with exsolved clinopyroxene are included in this subtype. IB5/IA2 composite xenoliths have orthopyroxenite in either intrusive or concordant relations to Type I peridotite host.

IB4 Olivine websterite--Three varieties (± brown spinel) are (1) allotriomorphic- or hypidiomorphic-granular to mosaic-equigranular clinopyroxene, orthopyroxene, and olivine, (2) coarse-grained porphyroclastic aggregates of kink-banded olivine within areas of hypidiomorphic to equigranular orthopyroxene and clinopyroxene, and (3) neoblastic olivine interstitial to coarse-grained subhedral pyroxene.

IB3 Websterite and clinopyroxenite--Discrete xenoliths of websterite (± olivine and brown spinel) range in size from 2 cm to 15 cm in diameter. Textures range from medium-grained allotriomorphic- and hypidiomorphic-granular to annealled mosaic-equigranular. Typically, fine exsolution lamellae of pyroxene (± spinel) are observed in orthopyroxene and clinopyroxene. Clinopyroxenite (± orthopyroxene, olivine, and brown spinel) and websterite (± olivine and brown spinel) form veins that cut IA1 lherzolite or layers concordant with foliation in IA2 lherzolite.

IB2 Clinopyroxene megacryst (discrete or relict)--Discrete megacrysts are 2-3 cm (angular or rounded) and exhibit extensive orthopyroxene exsolution. Relict megacrysts are partially recrystallized to secondary websterite (± olivine and brown spinel) and olivine websterite (± brown spinel) having allotriomorphic-granular to mosaic-equigranular texture and having exsolved and xenomorphic intergranular brown spinel. One large (15 cm) websterite crystal has a core containing a 4 cm exsolved "megacryst-like" clinopyroxene.

GENERAL DESCRIPTION AND OCCURRENCE OF HUTAYMAH TYPE I/TYPE II (TRANSITIONAL) PYROXENITE

Variants within the Hutaymah anhydrous pyroxenite suite transcend traditional group affiliations of either Type I (Cr-Mg rich) or Type II (Al-Ti rich). Texture and modal composition are gradational between Type II igneous pyroxenite and Ca-poor, Mg- and Cr-rich (Type I?) clinopyroxenite (fig. 4). Like IB pyroxenite, this transitional group is found only in tuff ring deposits and is classified as an undivided Type I pyroxenite (IB1). Transitional pyroxenite is very dark green (nearly black) and ranges from fine to coarse granular in hand specimens. Rare Type IB1 clinopyroxene megacrysts (about 3 cm) are distinctly greener than similar Type IIA1 megacrysts.

Type I/Type II transitional anhydrous igneous pyroxenite

IB1 Transitional clinopyroxenite, undivided--Clinopyroxene megacrysts are dark greenish brown, fractured, unexsolved, and are not twinned. Fine-grained (1-2 mm) equigranular-hypidiomorphic clinopyroxenite contains twinned clinopyroxene (± orthopyroxene). Medium- to coarse-allotriomorphic granular clinopyroxenite commonly has unexsolved, twinned clinopyroxene and may have poikilitically enclosed euhedral to rounded olivine. Allotriomorphic-granular olivine-clinopyroxenite contains as much as 10 percent of kink-banded, adcumulate-like olivine amidst unexsolved and commonly twinned clinopyroxene. Dark-green-brown spinel (less than 1 per cent) occurs as an interstitial xenomorphic phase in more granulated samples. In some samples, complex clinopyroxene exsolution processes are revealed by the textural gradation between lamellar and symplectic to poikilitic-like clinopyroxene-orthopyroxene intergrowths. This recrystallization texture may be attributed to in situ, high temperature subsolidus deformation of IB1 material (Boland and Otten, 1985)

GENERAL DESCRIPTION AND OCCURRENCE OF HUTAYMAH TYPE II XENOLITHS AND MEGACRYSTS

Type II xenoliths and megacrysts are common in Hutaymah basalt and ubiquitously associated with basaltic tuff deposits. While some Type II xenoliths might be readily interpreted as products of cumulus crystallization from host-type magmas at various depths, this group exhibits a range of chemical and petrologic characteristics which reflect more complex origins. Type II xenoliths range in lithology from amphibolite to an array of pyroxenitic rocks including clinopyroxenite, wehrlite, websterite, and orthopyroxenite (± garnet, green or black pleonaste spinel, sapphirine, calcic plagioclase, kaersutite, and minor sulfide, oxide, and CO_2 inclusions). Commonly observed Type II megacrysts are black aluminous clinopyroxene, black pleonaste spinel, and brown kaersutitic amphibole. There is an overlap of textural and mineralogic characteristics between Type II oikocrystic megacrysts and igneous xenoliths. Hydrous Type II inclusions range from metasomatized anhydrous rocks to primary precipitates from H_2O-rich alkaline basalt. Type II anhydrous pyroxenite xenoliths display a wide range of textures and mineral chemistry, reflecting primary igneous crystallization, meta-igneous annealling, or extensive metamorphic subsolidus recrystallization. Several varieties of Type II composite xenoliths are present at some Hutaymah tuff rings. Type I/II composites comprise 0.5- to 5-cm-wide Type II veins (amphibolite, igneous pyroxenite, or meta-igneous pyroxenite) in Type IA spinel lherzolite. Intratype composites of the Type II suite result from either primary layering (due to fractional settling or vein plating) or intrusive relationships between different Type II lithologies.

Type II classification

Type II xenoliths are divided into Type IIA and Type IIB subtypes, based on distinctive aspects of either igneous or metamorphic affinities, respectively. Further divisions are based on distinct variations in texture and mineralogy. Type IIA anhydrous igneous pyroxenite and wehrlite have characteristic Ca-poor and Al- and Ti-rich clinopyroxene (fig.4) and primary (or relict) igneous textures. Textures reflecting late-stage processes of recrystallization over a range of pressure (± plagioclase) at both above and below solidus temperatures and internal brecciation due to heating and depressurization are common in Type IIA inclusions. The Type IIB group comprises meta-igneous (annealed-cumulate) pyroxenite and metamorphic (granulite) pyroxenite. These all have Ca-rich clinopyroxene that is generally Al-depleted relative to Type IIA pyroxenite with a comparable range of Mg and Cr contents (fig. 4). Type IIB xenoliths are all anhydrous. Pyroxene chemistry is consistent with the observed variation in pyroxene exsolution and intergranular reaction products. There is complete textural gradation between spinel-free orthopyroxenite and websterite, xenomorphic-green-spinel websterite (± plagioclase, olivine, sapphirine, and garnet), and porphyroblastic-granular garnet-pyroxenite. Overall, the petrogenesis of IIB xenoliths can be attributed to processes of in situ recrystallization and deformation during cooling at variable depths. Subtype IIC refers to hydrous Type IIA inclusions and is divided into amphibole megacryst, amphibolite, and amphibole-pyroxenite varieties. General characteristics of distinct Type II variants follow.

Type II xenoliths

Subtype IIA--Anhydrous igneous pyroxenite and wehrlite

IIA1 Clinopyroxene megacrysts--Typically 2 to 6 cm, angular to ovoid inclusions having a black, vitreous luster along fresh conchoidally fractured surfaces. Weathered surfaces are brown to black, lusterless, smooth or "knobby" (if oikiocrystic). Most megacrysts are extensively fractured and contain a variable population of both primary and secondary intracrystalline phases. Megacrysts having chadacrysts of olivine and(or) black pleonaste spinel are transitional toward adcumulate clinopyroxenite and wehrlite.. Heterogeneous sulfide-oxide blebs are common and often occur in echelon patterns. Fluid inclusions (± vapor and crystals) are present in many specimens and are clustered in curviplanar surfaces adjacent to intramegacryst reaction zones or less frequently are isolated inclusions. Clinopyroxene twinning and orthopyroxene exsolution are scarce. Megacrysts exhibiting partial granulation and recrystallization are similar to allotriomorphic to granulitic IIA2 clinopyroxenite.

IIA2 Clinopyroxenite--Black, medium- to coarse-granular hand specimens range in size to as much as 20 cm in diameter. Larger specimens (larger than 10 cm) are black and vitreous and are dominated by "megacryst-like" clinopyroxene. Primary accessory phases include black pleonaste spinel and olivine or orthopyroxene. Primary textures range from coarse-grained (0.5-2 cm) allotriomorphic-granular (adcumulate) to medium-grained (1-3 mm) hypidiomorphic-granular (orthocumulate) and are variably overprinted by late-stage granulation and reaction. Clinopyroxene is infrequently twinned and rarely exsolved. Composite association is only as a clinopyroxenite vein (1 cm wide) crosscutting a Type IA lherzolith.

IIA3 Wehrlite and olivine-rich clinopyroxenite--Similar in most respects to the textural range of olivine-bearing Type IIA2 clinopyroxenite but comprises samples with greater than 50 volume percent olivine and a smaller size range (generally less than 5 cm and rarely as much as 10 cm). Black pleonaste spinel is ubiquitous and olivine may be kink banded in coarse-grained adcumulate to allotriomorphic samples.

IIA4 Websterite--Black-brown, medium-size (3-10 cm), granular xenoliths. Textures are medium-grained (0.5-1 mm) hypidiomorphic-equigranular (orthocumulate) and rarely coarse-grained (5-10 mm) allotriomorphic (adcumulate). Black pleonaste spinel is a common accessory phase. Both orthopyroxene and clinopyroxene are generally exsolution free and some clinopyroxene is twinned.

IIA5 Fe-rich clinopyroxenite--Rare, granular, dark-green to black clinopyroxenite (± orthopyroxene) found as discrete xenoliths (less than 7 cm) and as intrusive veins (about 5 mm wide) in Type IA1 lherzolite. Clinopyroxene is distinctly Fe rich in comparison to other Type IIA inclusions. Textures are variable and include (1) medium-grained (1-2 mm) hypidimorphic-equigranular, twinned and untwinned, clinopyroxene with 2 cm clinopyroxene and porphyroclasts of identical composition, (2) equigranular to porphyroclastic clinopyroxene with exsolved and recrystallized orthopyroxene, and (3) composite veins containing allotriomorphic unexsolved and typically twinned clinopyroxene (1-2 mm).

Subtype IIC--Hydrous xenoliths and megacrysts

IIC1 Amphibole clinopyroxenite--Brown kaersutitic amphibole-bearing Type IIA xenoliths and clinopyroxene megacrysts with intracrystalline kaersutite intergrowths (less than 10 percent). Kaersutite having subhedral or xenomorphic morphology occurs as rims around pyroxene and intergranular, black pleonaste spinels in both coarse allotriomorphic-granular and hypidiomorphic-equigranular pyroxenite. Equigranular kaersutite pyroxenite occurs in composite association with IIC3 amphibolite.

IIC2 Amphibole megacrysts--Dark-brown to black, 2-4 cm, prismatic to angular or rounded kaersutitic amphibole megacrysts, frequently displaying obtuse cleavage angle. Megacrysts range from translucent (± exsolved spinel and spherical microlite-bearing inclusions) to nearly opaque due to pervasive partial melting and oxide precipitation.

IIC3 Amphibolite--Dark-brown to black, granular xenoliths, as large as 12 cm, ranging in texture and lithology from medium-grained, granular, amphibole-rich pyroxenite (IIC1) to coarse-grained (0.5-2 cm) allotriomorphic granular kaersutite (± spinel). Coarse-grained amphibolite occurs in composite association with Type IA lherzolite and Type IIC1 pyroxenite.

Subtype IIB--Anhydrous meta-igneous and metamorphic pyroxenite

IIB1 Websterite--Dark-brown to black, 3-5 cm in size, medium-grained (1-3 mm) to coarse-grained (3-10 mm), granular xenoliths. All have no spinel and have variable amounts of exsolution in pyroxene. Textural variants include allotriomorphic equigranular to hypidiomorphic equigranular, and poikiloblastic. Some samples contain a pervasive intergranular network-vein material comprising euhedral green spinel and pyroxene microlites (± glass). These may be transitional to Type IIB3 green-spinel websterite. Poikiloblastic samples have exsolution-derived subhedral to round inclusions and overgrowths of clinopyroxene and orthopyroxene and may have resulted from high-temperature subsolidus deformation. Type IIB1 xenoliths may represent variably exsolved, deformed and recrystallized equivalents of Type IIA pyroxenite.

IIB2 Orthopyroxenite--Dark-brown to black, 3-7 cm in size, coarse-grained (5-10 mm), granular xenoliths. Most have no spinel and are allotriomorphic- to hypidiomorphic-equigranular intergrowths of orthopyroxene with less than 10 percent clinopyroxene. In some samples, clinopyroxene occurs as an intergranular phase at junctions of larger orthopyroxene crystals that are variably deformed and exsolved. This group is similar to IIB1 websterite.

IIB3 Green-spinel websterite--Dark-green to black, 5-11 cm in size, layered and nonlayered, medium-grained (1-3 mm) granular xenoliths. Clinopyroxene and orthopyroxene having variable amounts of fine-lamellar pyroxene (± spinel) exsolution are typically in an allotriomorphic- to hypidiomorphic-equigranular textural association. Pyroxene of the originally adcumulate to orthocumulate websterite often has exsolution-free rims and has developed late-stage intergranular xenomorphic green spinel and unexsolved orthopyroxene during annealling under near- to below-solidus conditions. Large specimens reveal 1- to 5-cm-thick gradational layers that are clinopyroxene-rich, orthopyroxene-rich, or spinel-rich, which are interpreted to represent variably annealled, primary-igneous layers produced by fractional-cumulate or vein-plating processes. The range of modal mineralogy in layers and in nonlayered samples is 45-55 percent clinopyroxene, 25-55 percent orthopyroxene, and 3-20 percent green spinel (± less than 2 percent sapphirine). In rare sapphirine-bearing xenoliths, sky-blue sapphirine occurs continuously along contacts between green spinel and pyroxene. In addition to intra-type composite relations in layered samples, green-spinel websterite occurs as a 5-cm-wide vein in Type IA1 lherzolite.

IIB4 Green-spinel olivine websterite--Dark-green to black 5-12 cm in size, medium (1-3 mm) to coarse-grained (as much as 2 cm) granular xenoliths. The medium-grained variety is hypidiomorphic- or mosaic-equigranular, and olivine is interstitial to exsolved orthopyroxene and clinopyroxene. This variety is observed in composite association with Type IA3 lherzolite. Coarse-grained samples comprise coarse-allotriomorphic intergrowths of large exsolved pyroxene crystals and kink-banded olivine and spinel crystals. They are variably granulated, and there is localized 1-3 mm equigranular-neoblastic pyroxene and olivine. Interstitial, xenomorphic, green spinel is present in all Type IIB4 xenoliths and is distinctly more brown in color than Type IIB3 green spinel. Type IIB4 clinopyroxene compositions overlap those in Type IB pyroxenite.

IIB5 Green-spinel plagioclase websterite--Rare, dark-green to black, as much as 6 cm in size, medium-grained (1-2 mm), granular xenoliths. Texture is allotriomorphic- to hypidiomorphic-equigranular. Plagioclase grains (less than 40 percent) are equant and bounded by an equal amount of clusters of similar size, variably exsolved clinopyroxene and orthopyroxene. Green spinel is an intergranular subhedral to xenomorphic phase. Overall texture suggests an annealed cumulate origin.

IIB6 Green-spinel garnet pyroxenite--Black, granular xenoliths ranging in size from 5 to 12 cm and generally medium-grained (1-4 mm). Textures are fundamentally similar to layered and nonlayered IIB3 green-spinel websterite but are more deformed. Garnet (calcic pyrope-almandine) is a subsolidus reaction product of pyroxene and pyroxene plus spinel. The mineralogy is 45-70 percent clinopyroxene, 7-30 percent orthopyroxene, 10-35 percent garnet, and 5-15 percent green spinel. Garnet occurs as xenomorphic crystals either surrounding or completely replacing green spinel; many are exsolved from clinopyroxene and some from orthopyroxene. In extensively granulated samples, premetamorphic textures are less recognizable and garnet is present as anhedral porphyroblasts, coarse exsolution blebs in pyroxene, and as network veins accumulated at pyroxene grain boundaries. Garnet is variably altered to kelyphite.

IIB7 Garnet pyroxenite (sparse spinel or no spinel)--Rare, dark-green-brown to black, coarse-granular (3-10 mm) xenoliths having a size range of 5-9 cm. The mineralogy is 45-75 percent clinopyroxene, 5-30 percent orthopyroxene, and 15-30 percent garnet (± traces of spinel). Coarse equigranular orthopyroxene and clinopyroxene have thick (as much as 0.5 mm) garnet-bearing exsolution lamallae. Xenomorphic garnet is prevalent at pyroxene grain junctions and forms a polygonal network surrounding coarse equigranular pyroxene.

HUTAYMAH COMPOSITE XENOLITHS

A composite xenolith is an individual sample composed of more than one distinct rock type. Both inter-type and intra-type composite xenoliths are present at Harrat Hutaymah. Rock types observed in "composite association" are summarized as follows (see previous descriptions for explanations of symbols):

Intratype I	Intratype II	Intertype I/II
IB5 vein in IA2 host	IIC3 vein in IIC1 host	IIA2 vein in IA2 host
IB5 layer in IA2 host	IIB3 layered (clinopyroxene and orthopyroxene rich)	IIA5 vein in IA1 host
IB3 vein in IA1 host		IIB3 vein in IA1 host
IB3 layer in IA2 host		IIB4 vein in IA3 host
IB4 inclusions in IB3 host		IIC3 vein in IA2 host

ACKNOWLEDGMENTS

The author thanks John Pallister for introducing him to Harrat Hutaymah; Robert Friar, as both pilot and field colleague; and his staff at the U.S. Geological Survey (USGS) Mineralogy and Petrology Laboratories, Jeddah, Saudi Arabia. Jim Budahn (USGS, Denver) performed instrumental neutron activation analysis of basalt samples. This work was supported in part by the Saudi Arabian Deputy Ministry for Petroleum and Mineral Resources through a cooperative work agreement with the USGS Reviews were provided by James Quick, Richard Moore, and James Cole (USGS Denver) and B. Carter Hearn (USGS, Reston).

REFERENCES

Boland, J.N., and Otten, M.T., 1985, Symplectitic augite; evidence for discontinuous precipitation as an exsolution mechanism in Ca-rich clinopyroxene: Journal of Metamorphic Geology, v. 3, p. 13-20.

Camp, V.E., Hooper, P.R., Roobol, M.J., and White, D.L., 1987, The Madinah eruption, Saudi Arabia; Magma mixing and simultaneous extrusion of three basaltic chemical types: Bulletin of Volcanology, v. 49, p. 489-508.

Camp, V.E., and Roobol, M.J., 1989, The Arabian continental alkali basalt province; part I., evolution of Harrat Rahat, Kingdom of Saudi Arabia: Geological Society of America Bulletin, v. 101, p. 71-95.

Cochran, J.R., 1983, A model for development of the Red Sea: American Association of Petroleum Geologists Bulletin, v. 67, p. 41-69.

Cole, J.C., and Hedge, C.E., 1986, Geochronologic investigation of Late Proterozoic rocks in the northeastern shield of Saudi Arabia: Ministry of Petroleum and Mineral Resources, Deputy Ministry for Mineral Resources, Jiddah, Kingdom of Saudi Arabia, Technical Record, USGS-TR-05-5, 42 p.

Coleman, R.G., 1984, The Red Sea; a small ocean basin formed by continental extensions and sea floor spreading: Proceedings of the 27th International Geological Congress, Moscow, v. 23, p. 93-121.

Coleman, R.G., Fleck, R.J., Hedge, C.E., and Ghent, E.D., 1977, The volcanic rocks of southwest Saudi Arabia and the opening of the Red Sea, in Hilpert, L.S., ed., Red Sea Research, 1970-1975: Saudi Arabian Directorate of Mineral Resources, Bulletin no. 22, p. 1-20.

Coleman, R.G., Gregory, R.T., and Brown, G.F., 1983, Cenozoic volcanic rocks of Saudi Arabia: U.S. Geological Survey Open-File Report OF-03-83, 82 p.

DuBray, E.A., 1984, Reconnaissance Geology of the Al Makhul quadrangle, Sheet 26/42 B, Kingdom of Saudi Arabia: Ministry of Petroleum and Mineral Resources, Deputy Ministry for Mineral Resources, Jiddah, Kingdom of Saudi Arabia, Open-File Report, USGS-OF-04-25, 40 p.

Fitch, F.H., 1980, Saudi Arabian stratigraphic lexicon: Saudi Arabian Deputy Ministry for Mineral Resources Technical Record DM-01-1, 273 p.

Frey, F.A., Prinz, M., 1978, Ultramafic inclusions from San Carlos, Arizona; petrologic and geochemical data bearing on their petrogenesis: Earth and Planetary Sciences Letters, v. 38, p. 129-176.

Ghent, E.D., Coleman, R.G., and Hadley, D.G., 1980, Ultramafic inclusions and host alkali olivine basalts of the southern coastal plain of the Red Sea, Saudi Arabia: American Journal of Science, v. 280-A, p. 499-527.

Harte, B., 1977, Rock nomenclature with particular relation to deformation and recrystallization textures in olivine-bearing xenoliths: Journal of Geology, v. 85, p. 279-288.

Harte, B., 1983, Mantle peridotite and processes--the Kimberlite sample, in Hawkesworth, C.J., and Norry, M.W., eds., Continental Basalts and Mantle Xenoliths: p. 46-91.

Irvine, T.N., and Baragar, W.R.A., 1971, A guide to the chemical classification of the common volcanic rocks: Canadian Journal of Earth Sciences, v. 8, p. 523-548

Johnson, P.T., 1983, A preliminary lithofacies map of the Saudi Arabian shield; an interpretation of the lithofacies and lithostratigraphy of the late Proterozoic layered rocks of Saudi Arabia (1:1,000,000) scale, in two sheets: Ministry of Petroleum and Mineral Resources, Deputy Ministry for Mineral Resources, Jiddah, Kingdom of Saudi Arabia, Technical Record RF-TR-03-2, 72 p.

Johnson, P.R., and Williams, P.L., 1984, Geology of the Precambrian rocks of the Jabal Habashi quadrangle, Sheet 26F, Kingdom of Saudi Arabia, with geographic map by Fuller, Fred J.: Ministry of Petroleum and Mineral Resources, Deputy Ministry for Mineral Resources, Jiddah, Kingdom of Saudi Arabia, Open-File Report USGS-OF-04-10, plate 1, 87 p.

Kellogg, K.S., 1984, Reconnaissance geology of the Rak quadrangle, sheet 27/42C, Kingdom of Saudi Arabia: Ministry of Petroleum and Mineral Resources, Deputy Ministry for Mineral Resources, Jiddah, Kingdom of Saudi Arabia, Open-File Report, USGS-OF-04-22, 36 p.

Kellogg, K.S., 1985, Root zone of the Late Proterozoic Salma Caldera, northeastern Arabian Shield, Kingdom of Saudi Arabia: Journal of Geophysical Research, v. 90. no. B13, p. 11,252-11,262.

LeBas, M.J., LeMaitre, R.W., Streckeisen, Albert, and Zanettin, B., 1986, A chemical classification of volcanic rocks based on the total alkali-silica diagram: Journal of Petrology, v. 27, pt. 3, p. 745-750.

McGuire, A.V., 1988, The mantle beneath the Red Sea margin; xenoliths from western Saudi Arabia: Tectonophysics, v. 150, p. 101-119.

Menzies, M.A., 1983, Mantle ultramafic xenoliths in alkaline magmas; evidence for mantle heterogeneity modified by magmatic activity, in Hawkesworth, C.J., and Norry, M.J., eds., Continental basalts and mantle xenoliths: Academic Press Inc., p. 92-110.

Mercier, J.C., and Nicholas, Adolph, 1975, Textures and fabric of upper mantle peridotites as illustrated by xenoliths from basalts: Journal of Petrology, v. 16, p. 454-487.

Nielson-Pike, J.E., and Schwarzman, E.C., 1976, Classification of textures in ultramafic xenoliths: Journal of Geology, v. 85, p. 49-61.

Pallister, J.S., 1984, Reconnaissance geology of the Harrat Hutaymah quadrangle, sheet 26/42 A, Kingdom of Saudi Arabia: Ministry of Petroleum and Mineral Resources, Deputy Ministry for Mineral Resources, Jiddah, Kingdom of Saudi Arabia, Open-File Report USGS-OF-04-46, 77 p.

Pallister, J.S., 1987, Magmatic history of Red Sea rifting; perspective from the central Saudi Arabian coastal plain: Geological Society of America Bulletin, v. 98, p. 400-417.

Pallister, J.S., Stacey, J.S., Fischer, L.B., and Premo, W.R., 1988, Precambrian ophiolites of Arabia; geologic settings, U-Pb geochronology, Pb-isotope characteristics, and implications for continental accretion: Precambrian Research, v. 38, p. 1-54.

Quick, J.E., and Bosch, P.S., 1989, Tectonic history of the northern Nabitah fault zone, Arabian shield, Kingdom of Saudi Arabia: Saudi Arabian Deputy Ministry for Mineral Resources Technical Record USGS-TR-08-02, 5 maps, 85 p.

Quick, J.E., and Doebrich, J.L., 1987, Geologic map of the Wadi Ash Shu'Bah quadrangle, sheet 26E, Kingdom of Saudi Arabia, Ministry of Petroleum and Mineral Resources, Deputy Ministry, Directorate General of Mineral Resources, Geoscience Map GM-108C, scale 1:250,000.

Richter, D.H., Allen, M.S., DuBray, E.A., Kleinkopf, M.D., Pallister, J.S., Raines, G.L., Smith, C.W., and Williams, P.L., 1984, Metallic-mineral assessment of the Jabal Habashi quadrangle, sheet 26F, Kingdom of Saudi Arabia: Ministry of Petroleum and Mineral Resources, Deputy Ministry for Mineral Resources, Jiddah, Kingdom of Saudi Arabia, Technical Record USGS-TR-04-8, 75 p.

Stoeser, D.B., and Camp, V.E., 1985, Pan African microplate accretion of the Arabian shield: Geological Society of America Bulletin, v. 96, p. 817-826.

Stoeser, D.B., and Elliott, J.E., 1980, Post-orogenic peralkaline and calc-alkaline granites and associated mineralization of the Arabian Shield, Kingdom of Saudi Arabia, in Evolution and mineralization of the Arabian-Nubian Shield: King Abdul Aziz University, Jiddah, Saudi Arabia, Institute of Applied Geology, Bull. 3, p. 1-23.

Streckeisen, Albert., 1973, Plutonic rocks; classification and nomenclature recommended by the IUGS subcommission on the systematics of igneous rocks: Geotimes, v. 26, p. 26-30.

Stuckless, J.S., Hedge, C.E., Wenner, D.G., and Nkomo, I.T., 1984, Isotopic studies of postorogenic granites from the northwestern Arabian shield, Kingdom of Saudi Arabia: Ministry of Petroleum and Mineral Resources, Deputy Ministry for Mineral Resources, Jiddah, Kingdom of Saudi Arabia, Open-File Report, USGS-OF-04-42, 40 p.

Vaslet, Denis, Kellogg, K.S., Berthiaux, Alain, Strat, Paul Le, and Vincent, Pierre-Louis, 1987, Geologic map of the Baq'A' quadrangle, sheet 27F, Kingdom of Saudi Arabia: Kingdom of Saudi Arabia, Ministry of Petroleum and Mineral Resources, Deputy Ministry for Mineral Resources, Geoscience Map GM-116C, scale 1:250,000.

Wilshire, H.G., and Shervais, J.W., 1975, Al augite and Cr diopside ultramafic xenoliths in basaltic rocks from the western United States: Physical Chemistry of the Earth, v. 9, p. 257-272.

Manuscript approved for publication, April 27, 1990

INTERIOR—GEOLOGICAL SURVEY, RESTON, VIRGINIA—1990

For sale by U.S. Geological Survey Map Distribution, Box 25286, Federal Center, Denver, CO 80225

Any use of trade names in this publication is for descriptive purposes only and does not imply endorsement by the U.S. Geological Survey